الجمهورية الجزائرية الديمقراطية الشعبية
**PEOPLE'S DEMOCRATIC REPUBLIC OF ALGERIA**

وزارة التعليم العالي و البحث العلمي
**MINISTRY OF HIGHER EDUCATION AND SCIENTIFIC RESEARCH**

جامعة عمار ثليجي بالأغواط
**UNIVERSITY AMAR TELIDJI OF LAGHOUAT**

كلية التكنولوجيا
**Faculty of Sciences and Technology**


Department of Electrical Engineering

Dissertation

Submitted in partial fulfillment of the requirements for Master degree in Automation

Option: Automation and Systems

Presented by **Bait Anfal Lina**

## Theme

# Flatness-based Control of a PEM Fuel Cell Air-Feed System

Jury:

| | | | |
|---|---|---|---|
| President | Ali Cheknane | Professor | University of Laghouat |
| Director | Mohamed Bougrine | MCB | University of Laghouat |
| Examiner | Mohammed Benmiloud | MCB | University of Laghouat |
| Examiner | Bachir Bendjedia | MCA | University of Laghouat |

*Juin 2024*

# Acknowldgement

First of all, I thank my great God who gave me the faith, willpower, and patience to be able to complete this thesis.

This work was carried out within the department of electrical engineering at Amar Telidji University of Laghouat, under the supervision of Dr. Mohamed Bougrine, Associate Lecturer at the University of Laghouat. I wish to express my profound and respectful gratitude to him for guiding my work with patience and diligence throughout the preparation of this thesis.

I would like to thank the president of the jury for the honor he has done me by accepting the chairmanship of the jury.

I am very grateful to Dr. Bachir Bendjedia, Dr.Hadj Aissa for agreeing to be part of my jury, thus showing their interest in this work.

Bait Anfal Lina

# Dedication

In the name of Allah, the Most Gracious, the Most Merciful.

I thank my great God, hoping He accepts it graciously and makes it solely for His pleasure. May it benefit everyone who reads it, serving as a source of knowledge and inspiration. Let it be a humble offering of gratitude for all my blessings.

To myself, I dedicate this achievement as a testament to my hard work, determination, and resilience. This journey, filled with challenges and triumphs, has fostered personal and professional growth. May this accomplishment be a stepping stone to greater endeavors and a reminder of what can be achieved through faith and dedication.

To my beloved family, thank you for your love, care, and unwavering support.

To my dear friends, thank you for your constant presence, shared memories, and inspiration.

To my esteemed professors, thank you for your ceaseless support and guidance. Your dedication has been a beacon of light, and I pray that Allah rewards you and grants you continued success and blessings.

To my esteemed supervisor, thank you for your tireless guidance and support. May Allah bless you abundantly.

Lastly, thank you to everyone who contributed with kind words or sincere advice. May Allah grant us all success and guidance.

# ملخص

هذه الدراسة تطور استراتيجية تحكم مبنية على التسطيح لضبط نسبة فائض الأكسجين ( $\lambda_{O2}$ ) في أنظمة خلايا الوقود. في البداية، يتم إنشاء نموذج مُقَلَّل من أربع حالات ونسخته المُعادَةَ الخطية حول نقطة التشغيل الاسمية، مما يُسلِّط الضوء على اختلافات كبيرة بين النماذج الخطية وغير الخطية تحت نقاط التشغيل المختلفة. بينما يُظهر التحكم المبني على التسطيح بناءً على النموذج الخطي تتبعًا مثاليًا ل $\lambda_{O2}$ ، يكشف تطبيقه على النموذج غير الخطي عن أخطاء كبيرة. تعزز دمج متحكم نسبيتكاملي (عي) الدقة عن طريق دمج خطأ $\lambda_{O2}$ ، مما يُؤكد دور استراتيجيات التحكم القوية في تحسين أداء خلايا الوقود.



الكلمات المفتاحية: تكنولوجيا الخلايا الوقود، التحكم المبني على الانسيابية، نقص الأكسجين، كفاءة الطاقة، استدامة الطاقة



# Abstract

This study develops a flatness-based control strategy for regulating the oxygen excess ratio ($\lambda_{O2}$) in fuel cell systems. Initially, a reduced four-state model and its linearized version are established, highlighting significant deviations between linear and nonlinear models under varying operational points. While flatness control based on the linear model shows perfect tracking of $\lambda_{O2}$, application to the nonlinear model reveals significant errors. Integration of a Proportional-Integral (PI) controller enhances precision by incorporating $\lambda_{O2}$ error, underscoring the role of robust control strategies in optimizing fuel cell performance.



**Keywords:** Fuel Cell, Flatness-Based Control, Nonlinear Dynamics, Proportional-Integral Controller, System Stability.

# Contents

**1 Background and Overview** **12**

1.1 Introduction To Polymer Electrolyte Membrane Fuel Cells (PEMFC) . . . . . 12

1.1.1 Introduction . . . . . 12

1.1.2 Historical Background . . . . . 12

1.2 General Overview of the Fuel Cell . . . . . 13

1.2.1 FUEL CELL . . . . . 13

1.2.2 Different types of proton exchange membrane : . . . . . 14

1.3 Fuel-Cell System . . . . . 15

1.3.1 Reactant Flow Subsystem : . . . . . 16

1.3.2 Heat and Temperature Subsystem . . . . . 16

1.3.3 Water Management Subsystem . . . . . 17

1.3.4 Power Management Subsystem . . . . . 17

1.3.5 Fuel Processor Subsystem . . . . . 17

1.4 Control system overview . . . . . 18

1.5 Fuel Cell Applications . . . . . 18

1.5.1 Stationary Applications . . . . . 19

1.5.2 Transport Applications . . . . . 19

1.5.3 Mobile Applications : . . . . . 20

1.6 Conclusion . . . . . 20

**2 Modeling of the PEM Fuel-Cell System** **21**

2.1 Introduction . . . . . 21

2.1.1 Fuel Cell System Model . . . . . 21
2.1.2 Dynamic States . . . . . 23
2.1.3 Non Linear Static Relations . . . . . 24
2.1.4 Input And Output In The Fuel Cells . . . . . 27
2.2 Fuel-cell Linearized Model . . . . . 27
2.2.1 Linearization principle . . . . . 27
2.2.2 Linearization Methodology . . . . . 28
2.3 Model validation . . . . . 30
2.3.1 Simulation around an operating point close to the reference . . . . . 30
2.3.2 Simulation around an operating point far from the reference . . . . . 33
2.3.3 Conclusion . . . . . 33

**3 Flatness Control of The FC air-feed subsystem 35**

3.1 Introduction . . . . . 35
3.2 Flatness Control . . . . . 36
3.3 Flatness of the Linear Satate space Representation . . . . . 36
3.4 Flatness of the Linear Model of the Fuel cell . . . . . 38
3.5 Trajectory Planning . . . . . 40
3.5.1 Polynominal Trajectory Generation . . . . . 40
3.5.2 Trajectory generation using Filters . . . . . 41
3.6 Simulation . . . . . 41
3.6.1 Fltaness-Based Control of the Linear Fuel cell . . . . . 44
3.6.2 Simulation with the nonlinear Fuel-cell model . . . . . 45
3.6.3 Modified Linear Flatness-based Control of PEMFC . . . . . 46
3.6.4 Conclusion . . . . . 47

# List of Figures


1.1 Schematic representation of the first fuel cell [15] . . . . . 13

1.2 Representative shematic of the Pemfc with its layers and working principle . . . . . 14

1.3 Different types of fuel cells with their reactions and operating temperature. [13] . . . . . 15

1.4 fuel cell system showing control inputs and outputs . . . . . 16

1.5 PEM Fuel-Cell Applications [7] . . . . . 18

1.6 Stationary Application . . . . . 19

1.7 Transport Application [9] . . . . . 19

1.8 Mobile Application of the Fuel-Cell . . . . . 20

2.1 Fuel Cell Reduced Model . . . . . 23

2.2 Response of the Nonlinear & Linearized Models for a fixed operating point . . . . . 31

2.3 Response of the Nonlinear & Linearized Models for a different operating point . . . . . 32

3.1 Trajectory Planning using filters . . . . . 41

3.2 Fatness control of Fuel cell Model . . . . . 43

3.3 Flat output lineair model . . . . . 44

3.4 states lineair control . . . . . 45

3.5 lamda O2 lineair model . . . . . 46

3.6 Flat output signals of the nonlinear model . . . . . 47

3.7 state signals of the nonlinear model . . . . . 48

3.8 $lambda_{O2}$ trajectory in the nonlinear model . . . . . 49

3.9 Flat output signal with the modified Flatness-based control . . . . . 49

3.10 $\lambda_{O2}$ signal with the modified flatness-based control . . . . . 50

3.11 Fatness control of Fuel cell Model with Flat Output Correction . . . . . 50

# List of Tables

3.1 Parameters of the FC used in the simulation . . . . . 43

# General Introduction

Proton Exchange Membrane Fuel Cells (PEMFCs) have emerged as a cornerstone technology in the quest for clean and efficient energy solutions, offering substantial benefits in terms of efficiency, scalability, and environmental impact. These fuel cells generate electricity through the electrochemical reaction between hydrogen and oxygen, with water and heat as the only byproducts, making them a highly attractive option for diverse applications. From portable power sources to large-scale power plants, and particularly in automotive applications, PEMFCs stand out due to their rapid start-up and responsive performance.

A critical challenge in Proton Exchange Membrane Fuel Cell (PEMFC) systems is addressing "oxygen depletion" during sudden increases in cell current. While conventional control methods such as Linear Quadratic Regulator (LQR) and Proportional-Integral (PI) controllers are commonly used, this research aims to optimize the FCS efficiency by increasing the concentration of $\lambda_{O_2}$, said the oxygen stoichiometry, using flatness control. Flatness control offers several advantages over traditional methods, it provides a deeper understanding of PEMFC system dynamics, particularly around its nominal operating point. A flatness control is designed with a trajectory planning feature to address the critical issue of oxygen depletion within the fuel cell, optimizing its performance and stability.

In this memoir, we delve into the intricacies of PEMFC technology across several chapters, each aimed at building a comprehensive understanding and addressing critical challenges. Chapter One provides a thorough overview of PEMFC technology, detailing the fundamental operating principles, components, and materials involved. We explore the core electrochemical processes that drive PEMFCs and discuss both the challenges and advancements in this field.

Chapter Two shifts focus to the modeling of the PEMFC. Accurate modeling is pivotal for predicting behavior and enhancing the efficiency of fuel cells. A simplified four-state nonlinear dynamic model that is valid under some assumptions is given in detail. Then a linearized four-state model is numerically

deduced. This one is compared with the original nonlinear model in two different operating points under feed-forward control.

Chapter Three is dedicated to the concept of flatness control in fuel cell systems (FCS). It provides the necessary ingredient of flatness control, and trajectory planning, for their application to the FC using its linear model. This chapter cantains the main contribution of this research, where we use a linear-model-based flat control to tackle the challenge of controlling a nonlinear fuel cell. We show how this is possible, and with great performance, by introducing a PI action to correct the linear estimation of the system's flat output

Finally, we conclude this work with a comprehensive summary and recommendations for future research. We highlight key findings, discuss their broader implications, and suggest directions for further exploration to overcome remaining obstacles in PEMFC development and deployment. Through this detailed investigation, we aim to contribute to the advancement of PEMFC technology, fostering its adoption as a viable and sustainable energy solution for the future.

# Chapter 1

# Background and Overview

## 1.1 Introduction To Polymer Electrolyte Membrane Fuel Cells (PEMFC)

### 1.1.1 Introduction

A fuel cell is a device that produces electricity through a chemical reaction between a fuel, such as hydrogen, and an oxidant, such as oxygen. The chemical energy from the fuel is converted to electrical energy, with water vapor and heat as byproducts. Fuel cells are often considered a cleaner and more efficient alternative to traditional methods of producing electricity, as they produce little to no greenhouse gas emissions. They are also versatile and can be used in a range of applications, including transportation, stationary power generation, and portable electronics, In this chapter, we write a brief history on the evolution of fuel cells. Their operating principle, types, general structure, system, and various application areas are then presented.

### 1.1.2 Historical Background

Fuel cells have a long history that can be traced back over 160 years . In 1800, scientists discovered the process of using electricity to decompose water into hydrogen and oxygen, a process known as electrolysis. In 1838, William Robert Grove created the first fuel cell by arranging two platinum electrodes with one

end of each immersed in a container of sulfuric acid and the other ends separately sealed in containers of oxygen and hydrogen. These efforts involve development of new materials, economical manufacturing processes, advanced equipment for supplying air and fuel, advanced power electronics for controlling the cell output, and comprehensive approaches for systems analysis and optimization. Fuel cells remained a subject of intense research and development throughout the 1900s, with researchers and manufacturers, energy companies, and regulatory agencies working to develop a wide range of fuel cell types and the infrastructure to support these new technologies. Today, fuel cells offer high efficiency, excellent part load performance, lower emissions of regulated pollutants, and a wide size range. They are modular, scalable, and offer high electrical conversion efficiencies at both design and part-load operation.[16]

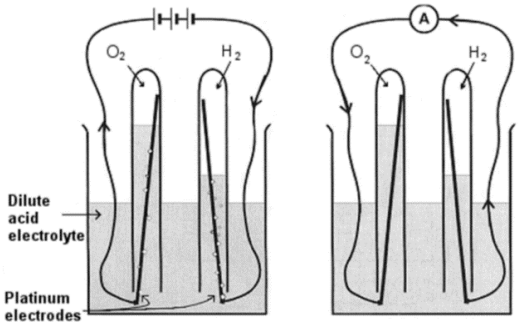


Figure 1.1: Schematic representation of the first fuel cell [15]

## 1.2 General Overview of the Fuel Cell

### 1.2.1 FUEL CELL

In today's era of heightened focus on sustainable energy solutions, fuel cells have garnered unprecedented interest. These innovative devices operate on the principle of electrochemical conversion, where fuel undergoes reactions such as the oxygen reduction reaction (ORR) and hydrogen oxidation reaction (HOR) to produce electricity. Specifically, in the Proton Exchange Membrane Fuel Cell (PEMFC) illustrated in Fig1.2, molecular hydrogen (H2) is delivered to the anode, where it oxidizes to form hydrogen ions (H+) and electrons ($e^{-1}$) according to the equation:

$$H_2 \rightarrow 2H^+ + 2e^{-1} \tag{1.1}$$

Concurrently, electrons traverse an external circuit towards the cathode, while hydrogen ions migrate through an acidic electrolyte. At the cathode, supplied oxygen (O2) combines with hydrogen ions and electrons to produce water:

$$O_2 + 4H^+ + 4e^- \rightarrow 2H_2O \tag{1.2}$$

, which overall can be represented as: $O_2 + 2H_2 \mapsto 2H_2O$. Notably, the sole byproduct of this electrochemical process is water. Hence, effective water management and optimal hydration levels, particularly within the bipolar plate channels, emerge as crucial factors influencing the efficiency and performance of PEMFCs.[12] [14]

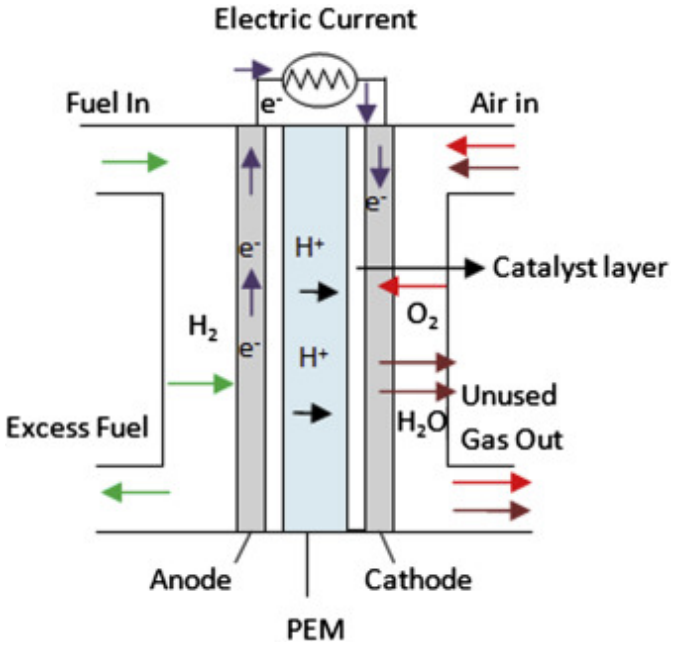


Figure 1.2: Representative shematic of the Pemfc with its layers and working principle

### 1.2.2 Different types of proton exchange membrane :

Since the dawn of fuel cell research and development initiatives, diverse classification methodologies have been utilized, delving into considerations such as fuel type, operating temperature (ranging from low to high), the composition of the electrolyte (liquid or solid) and system geometry. Presently, the scientific community has rallied around a classification paradigm centered on electrolyte type. The choice of electrolyte and fuel not only shapes electrode reactions and ion migration within the electrolyte but also

dictates the operational temperature of the cell. Six distinct categories of fuel cells have emerged:

- Phosphoric Acid Fuel Cells (PAFC).
- Alkaline Fuel Cells (AFC).
- Solid Oxide Fuel Cells (SOFC).
- Molten Carbonate Fuel Cells (MCFC).
- Direct Methanol Fuel Cells (DMFC).
- Proton Exchange Membranes Fuel Cells (PEMFC).

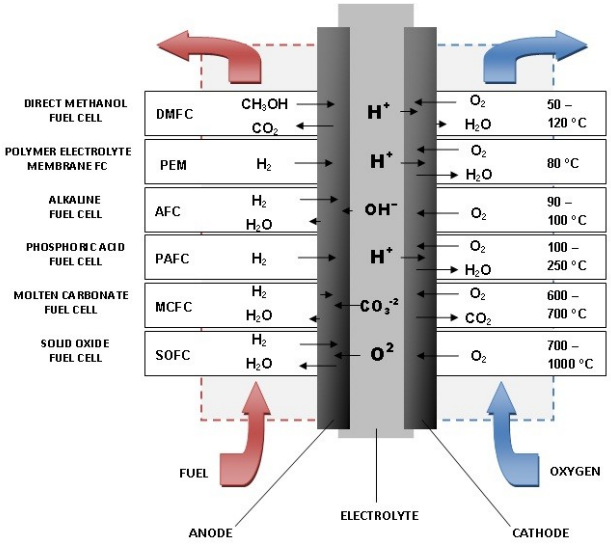


Figure 1.3: Different types of fuel cells with their reactions and operating temperature. [13]

## 1.3 Fuel-Cell System

fuel cell system is an electrochemical device that converts the chemical energy of a gaseous fuel directly into electricity. The fuel cell system requires external storage of reactants, usually hydrogen and oxygen or air, with oxygen typically taken from atmospheric air. The minimal components required for a pressurized fuel cell engine are a hydrogen supply system to the anode, an air supply system to the cathode, de-ionized water serving as a coolant in the stack cooling channel, and de-ionized water supply to the humidifier to humidify the hydrogen and the air flows. The system consists of four main subsystems, namely, reactant

supply, heat and temperature, water management, and power management subsystems. Fuel cell systems are widely regarded as a potential alternative stationary and mobile power source, complementing heat engines and reducing dependence on fossil fuels. [13]

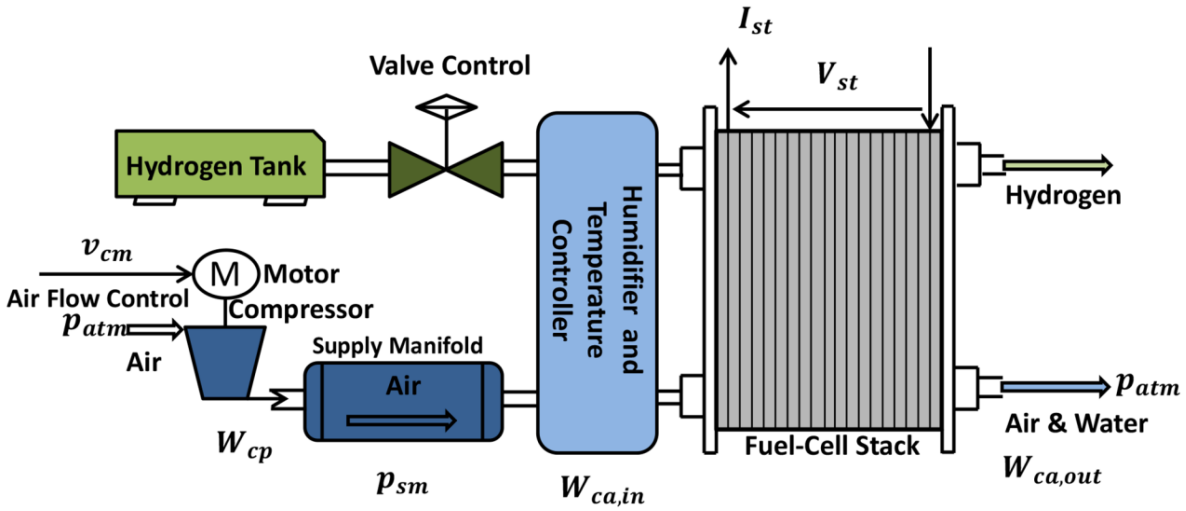


Figure 1.4: fuel cell system showing control inputs and outputs

### 1.3.1 Reactant Flow Subsystem :

The reactant flow subsystem consists of two loops: the hydrogen supply and air supply loops. The hydrogen and air flows are adjusted using the valve and compressor motor commands, respectively, to ensure fast transient responses and to minimize auxiliary power consumption. The non-minimum phase behavior of the fuel cell power output to changes in compressor motor input limits the closed-loop bandwidth of this loop.

### 1.3.2 Heat and Temperature Subsystem

The Heat and Temperature Subsystem in a fuel cell system includes components like the fuel cell stack cooling system and reactant temperature system. It manages heat generated during operation, cooling the stack efficiently to maintain optimal performance. Proper thermal management is crucial for fast warm-up, preventing stack temperature overshoot, and ensuring low auxiliary fan and pump power.[13]

### 1.3.3 Water Management Subsystem

The Water Management Subsystem in a fuel cell system is responsible for maintaining hydration of the polymer membrane and balancing water usage within the system. It regulates the amount of reactant flow and water injected into the anode and cathode flow streams to ensure optimal membrane humidity. Dry or flooded membranes can lead to high polarization losses, affecting fuel cell performance.[13]

### 1.3.4 Power Management Subsystem

The power management subsystem controls the power drawn from the fuel cell stack. Its goal is to ensure that the net power extracted from the stack follows the power demand, while maintaining the fundamental variables within desirable ranges. Without considering power management, the load current can be viewed as a disturbance to the fuel cell system. The majority of the parasitic power is caused by the air compressor, which is why it is the only parasitic loss considered in the study. For certain stack currents, the stack voltage increases with increasing air flow rate to the stack since the cathode oxygen partial pressure increases. [13]

### 1.3.5 Fuel Processor Subsystem

The significance of the fuel processor subsystem within the fuel cell system is underscored by the current deficiencies in hydrogen refueling, distribution, and storage infrastructure. To address this challenge, various fuel sources such as methanol, gasoline, and natural gas can be harnessed. The fuel processor subsystem is a sophisticated assembly comprising several integral components and processes, including hydro-desulfurization (HDS), catalytic partial oxidation (CPOX), water gas shift (WGS), and preferential oxidation (PROX). These processes collectively facilitate the conversion of carbon-based fuels into hydrogen [1]. However, the intricate interplay among these components, coupled with numerous control actuators, exacerbates the complexity of the control problem [10]

## 1.4 Control system overview

As presented in the previous paragraphs, we can see that the FC auxiliaries are highly interdependent and that this makes the Pem system difficult to control. It is therefore essential to develop a control system to ensure a good level of performance. This system consists of the following elements:

1) The air compressor control system whose purpose is to provide accurate flow depending on the load.

2) The hydrogen tank electrovalve control system, so as to manage the pressure at the inlet of the anode.

3) The pump control system that operates the water cooling system of the FC, or the control system of a fan in case of air cooling.

4) The control system of the pump feeding the humidification circuit.

5) The Converter Control System for Energy Management [10]

## 1.5 Fuel Cell Applications

Fuel cells can be used in almost any situation where electricity is required. Batteries are generally classified into three categories: stationary applications, transport applications and mobile applications.

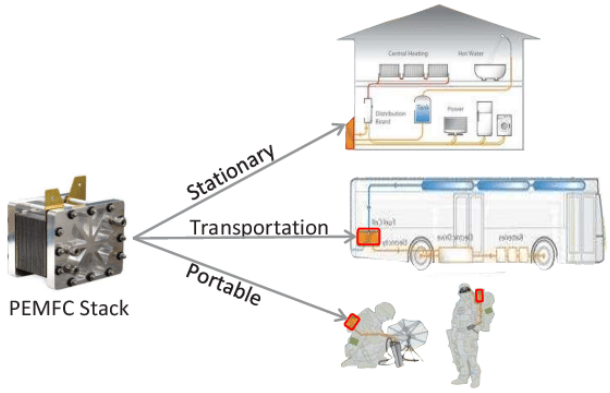


Figure 1.5: PEM Fuel-Cell Applications [7]

### 1.5.1 Stationary Applications

In this field, fuel cells are used to produce electricity and distribute it through a network. There are two areas of application: collective production, where the power ranges from 200kW to some MW, and domestic production, in which the power varies from 2 to 7kW. A large number of demonstration plants with power ranging from 1 kW for individual houses to a few hundred kW for residential buildings have been installed in different countries .The most commonly used batteries are those with a high operating temperature (SOFC, MCFC), where the use of the heat released for heating and the production of water vapour allows for maximum energy efficiency [4].

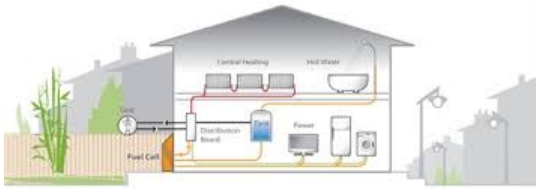

Figure 1.6: Stationary Application

### 1.5.2 Transport Applications

Transport was the area of application that led to the development of fuel cells in the early 1990s Two quite different subfamilies are distinguished depending on whether it is to equip a light vehicle or a heavy vehicle. This area requires that the battery to be used is ready for use in the shortest possible time, has a long service life and has an acceptable volume and mass power density. Su is suitable for batteries that have a low operating temperature, especially PEMFC batteries.[8]

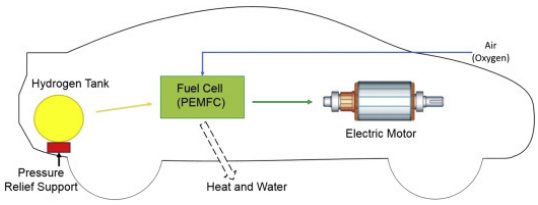


Figure 1.7: Transport Application [9]

### 1.5.3 Mobile Applications :

In mobile applications, it concerns mobile phones and laptops. The user recharges his laptop like a briquet or ink pen, in seconds, and each recharge gives 3 to 5 times more power than a current battery, for the same load. The most widely used batteries in this field are DMFC type. [8]

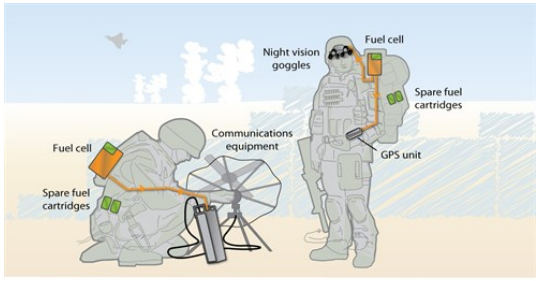


Figure 1.8: Mobile Application of the Fuel-Cell

## 1.6 Conclusion

In conclusion, fuel cells are a promising technology that offers a cleaner and more efficient alternative to traditional methods of producing electricity. They have a long history, spanning over 160 years, and have since evolved to include a range of fuel cell types and applications. Among them, Polymer Electrolyte Membrane Fuel Cells (PEMFCs) are widely used due to their high efficiency, low emissions, and versatility. To ensure optimal performance, fuel cells require proper management of reactant flow, heat and temperature, water, and power. While there are challenges to implementing fuel cell technology, such as the need for infrastructure for hydrogen refueling and distribution, fuel cells have shown promise in various applications, including stationary, transport, and mobile. With ongoing research and development efforts, fuel cells have the potential to revolutionize the energy industry. In the following chapter, we will discuss the modeling of fuel cell systems, which is an essential tool to optimize the design, control, and operation of fuel cells.

# Chapter 2

# Modeling of the PEM Fuel-Cell System

## 2.1 Introduction

The main goal of fuel cell modeling is to gain a better understanding of the physical phenomena involved and design an automatic system for air-feed subsystem control. As the control purpose is related to the cathode part of the FC system, in this chapter, we cover the modeling of the cathode part of the fuel cell system. We give a special insight to three interacting sub-models: the cathode flow, the supply manifold, and the compressor motor.

The stack voltage is determined by various factors, including stack current, cell temperature, air pressure, oxygen and hydrogen partial pressures, and membrane humidity. The model incorporates transient behaviors crucial for integrated control design and analysis.

### 2.1.1 Fuel Cell System Model

We consider a fuel cell stack with active cell area of $A_{fc} = 280\text{cm}^2$ and $n = 381$ number of cells with 75 kW gross power output that is applicable for automotive and residential use. The performance variables for the FC power system are (i) the stack voltage $v_{st}$ that has a direct influence on the stack power generated, $P_{fc} = v_{st} \times I_{st}$ when a load current $I_{st}$ is drawn from the stack, and (ii) the oxygen excess ratio $\lambda_{O_2}$ in the cathode that indirectly ensures adequate oxygen supply to the stack. Stack voltage is calculated as the product of the number of cells and cell voltage $v_{st} = n \times v_{fc}$. The combined effect of

thermodynamics, kinetics, and ohmic resistance determines the output voltage of the cell, as defined by :

$$v_{fc} = E - v_{act} - v_{ohm} - v_{conc} \tag{2.1}$$

Where $E$ is the open circuit voltage, $v_{act}$ is the activation loss, $v_{ohm}$ is the ohmic loss, and $v_{conc}$ is the concentration loss. The detailed formulation of the FC voltage, also known as polarization characteristic can be found in [13]. The voltage of a fuel cell, when in a steady state, is dependent on various factors such as the current density, oxygen and hydrogen partial pressures, cathode pressure, temperature, and humidity. Although the electrochemical reaction is assumed to be instantaneous and the capacity of the electrode double layer is negligible, the fuel cell voltage exhibits a dynamic behavior due to the fluctuating variables of the stack. Different cathode pressures and stack temperature conditions are shown to affect stack polarization in equation (2.1) Flow control is an essential aspect of operating a fuel cell system, and it primarily involves regulating the total cathode pressure ($p_{ca}$), oxygen pressure ($p_{O2}$), and oxygen excess ratio ($\lambda_{O_2}$) in the cathode. The parameter ($\lambda_{O_2}$) measures the ratio of oxygen supplied to oxygen consumed, and it is a crucial indicator of reactant utilization. In this context, each variable related to air supply and stack performance is defined. Precise control of reactant flow helps to reduce transient voltage excursions in the stack. However, the flow dynamics of hydrogen and oxygen reactants are also influenced by pressure dynamics through flow channels, manifolds, and orifices. Sufficient flow of oxygen and hydrogen into the fuel cell stack is necessary to prevent nitrogen films from covering the electrochemical surface and creating stagnant vapor. The fuel cell's load (current) will vary depending on The stack voltage ranges from 220 V to 350V, depending on the load (current) drawn from the fuel cell and the air supply to the fuel cell. A compressor that has a maximum power of 15 kW is used to supply the air. The compressor delivers 95 g/sec of air flow and 3.5 atm of pressure rise at its maximum rotating speed of 100 kRPM. When the maximum current is pulled ($I_{max} = 320$A), the maximum compressor air flow is double that which is required to replace the oxygen consumed from the stack. The current at which the highest possible FC power is obtained is known as the maximum FC current. Utilizing the fuel cell to generate greater current leads to rapid decrease of the stack voltage, and thus power due to concentration losses.

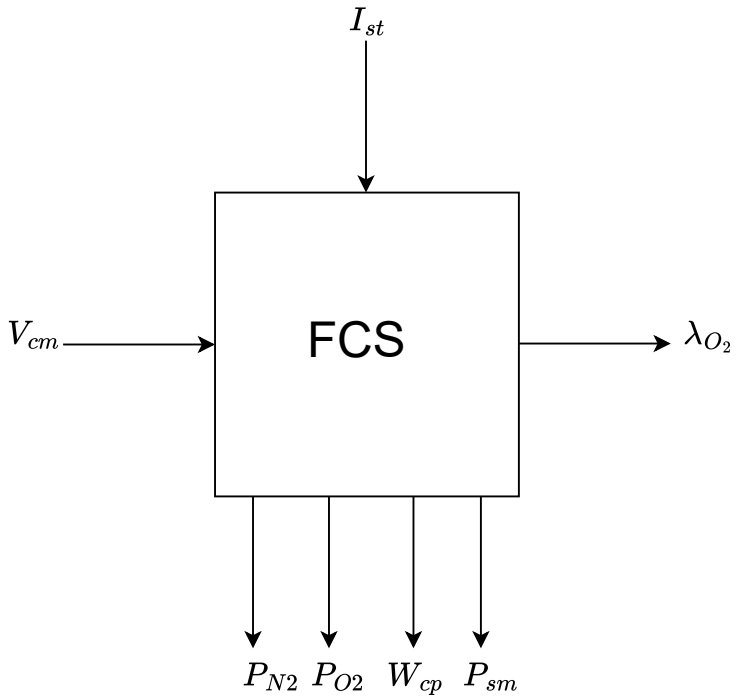


Figure 2.1: Fuel Cell Reduced Model

### 2.1.2 Dynamic States

To better understand the rapid dynamics of integrating a fuel cell with a DC/DC converter, we have implemented several simplifications and adjustments, particularly concerning air dynamics. These simplifications are based on the following assumptions:

(1) All gases adhere to the ideal gas law.

(2) The temperature of the air within the cathode is equal to the overall stack temperature, which matches the coolant temperature exiting the stack.

(3) The properties of the flow exiting the cathode, such as temperature and pressure, are assumed to match those within the cathode and are the primary factors influencing the reaction at the catalyst layers in the membrane.

(4 )The gases in both the anode and cathode are fully humidified, with any water in the cathode existing solely as vapor. Any excess water is converted to liquid and removed from the channels.

(5) Flooding in the gas diffusion layer is not considered.

(6) The flow channel and the gas diffusion layer are treated as a single volume, ignoring any spatial

variations.

The fuel cell is designed to supply power to external and auxiliary loads via its bus. It is crucial to maintain ideal humidity and temperature levels, although controlling these factors can be challenging. In the following section, we will outline the dynamic states of the model and describe the nonlinear connections between inputs, states, and outputs for control purposes. The mass continuity of oxygen and nitrogen inside the cathode volume, combined with the ideal gas law, yields:

$$\frac{dp_{O2}}{dt} = \frac{RT_{st}}{M_{O_2}V_{ca}}(W_{O_2,in} - W_{O_2,out} - W_{O_2,rct}) \tag{2.2}$$

$$\frac{dp_{N2}}{dt} = \frac{RT_{st}}{M_{N_2}V_{ca}}(W_{N_2,in} - W_{N_2,out}) \tag{2.3}$$

where $V_{ca}$ is the lumped volume of cathode, $R$ is the universal gas constant, and $M_{O_2}$ and $M_{N_2}$ are the molar mass of oxygen and nitrogen, respectively.

The rate of change of air pressure in the supply manifold, which connects the compressor with the fuel cell (as shown in Figure 2.2), depends on the compressor flow into the supply manifold $W_{cp}$, the flow out of the supply manifold into the cathode $W_{ca}$,and the compressor flow temperature $T_{cp}$:

$$\frac{dp_{sm}}{dt} = \frac{RT_{cp}}{M_a atm V_{sm}}(W_{cp} - W_{ca,in}) \tag{2.4}$$

where $V_{sm}$ is the supply manifold volume and Ma,atm is the molar mass of atmospheric air. The compressor motor state is associated with the rotational dynamics of the motor through thermodynamic equations. A lumped rotational inertia is used to describe the compressor with the compressor rotational speed $w_{cp}$ [11, 5].

$$\frac{d\omega_{cp}}{dt} = \frac{1}{J_{cp}}(\tau_{cm} - \tau_{cp}) \tag{2.5}$$

### 2.1.3 Non Linear Static Relations

The nonlinear relations connecting the dynamic states (pressure and rotational speed) are represented by the right-hand side of equations (2.2) to (2.4). The inlet mass flow rates of oxygen $W_{O_2,in}$ and nitrogen $W_{N_2,in}$ are derived from the inlet cathode flow $W_{ca,in}$ as follows:

$$W_{O_2,in} = \frac{x_{O_2,atm}}{1 + w_{atm}} W_{ca,in} \tag{2.6}$$

$$W_{N_2,in} = \frac{1 - x_{O_2,atm}}{1 + w_{atm}} W_{ca,in} \tag{2.7}$$

where $x_{O_2,atm}$ is the oxygen mass fraction of the inlet air given by:

$$x_{O_2,atm} = \frac{Y_{O_2,atm} M_{O_2}}{Y_{O_2,atm} M_{O_2} + (1 - Y_{O_2,atm}) M_{N_2}} \tag{2.8}$$

Here $Y_{O_2,atm} = 0.21$ represents the molar ratio of oxygen in the atmosphere,and $\omega_{atm}$ is the humidity ratio of the inlet air:

$$\omega_{atm} = \frac{M_v}{Y_{O_2,atm} M_{O_2} + (1 - Y_{O_2,atm}) M_{N_2}} \frac{Q_{atm} p_{sat}}{p_{atm} - Q_{atm} p_{sat}} \tag{2.9}$$

where $p_{\text{sat}} = p_{\text{sat}}(T_{\text{st}})$. is vapor saturation pressure and atm is the relative humidity at ambient conditions which is preset to the average value of 0.5. The supply manifold model describes the mass flow rate from the compressor to the outlet mass flow. A linear flow-pressure relationship is assumed due to the small pressure difference between the supply manifold and the cathod

$$W_{ca,in} = k_{ca,in} \left( p_{sm} - p_{ca} \right) \tag{2.10}$$

where $k_{ca,in}$ ,in is the supply manifold orifice flow constant, and the spatially invariant cathode press is the sum of the partial pressures pca of oxygen, nitrogen, and vapor. The rate of oxygen consumption $W_{O_2,rct}$ in (**??**) from the stack current Ist is given by;

$$W_{o_2,\text{ret}} = M_{o_2} \frac{n I_{\text{gt}}}{4F} \tag{2.11}$$

where $n$ is the number of cells in the stack and $F$ is the Faraday number. The outlet mass flow rate of oxygen $W_{O_2,out}$ and nitrogen $W_{N_2,out}$ used in (2.2) and (2.3) are calculated from the mass fraction of

oxygen and nitrogen in the stack after the section

$$W_{O_2,\text{out}} = \frac{M_{O_2} p_{O_2}}{M_{O_2} p_{O_1} + M_{N_2} p_{N_2} + M_v p_{\text{sat}}} W_{\text{ca,cut}} \tag{2.12}$$

$$W_{N_1,\text{out}} = \frac{M_{N_2} p_{N_2}}{M_{O_2} p_{O_2} + M_{N_2} p_{N_2} + M_v p_{\text{sat}}} W_{\text{ca,out}} \tag{2.13}$$

The total flow rate at the cathode exit $W_{\text{ca, out}}$ is calculated using the nozzle flow equation due to the significant pressure difference between the cathode and the ambient pressure

$$W_{\text{ca,out}} = C_D A_T p_{\text{ca}} \sqrt{\frac{RT_{\text{st}}}{\gamma}} \left(\frac{2}{\gamma+1}\right)^{\frac{\gamma+1}{2(\gamma-1)}} \quad \text{for} \quad \frac{p_{\text{atm}}}{p_{\text{ca}}} \leq \left(\frac{2}{\gamma+1}\right)^{\frac{\gamma}{\gamma-1}} \tag{2.14}$$

where $\gamma$ is the ratio of the specific hest capacities of the sir, $C_D$ is the discharge coefficient of the nozzle, $A_T$ is the opening area of the noczle.

The compressor flow $W_{cp}$ is modeled by applying the Jensen and Kristensen nonlinear fitting method [13] as functions of the pressure ratio $p_{sm}/p_{\text{atm}}$ , the upstream temperature $T_{\text{atm}}$ , and the compressor rotational speed $\omega_{\text{ep.}}$ . The temperature of the air leaving the compressor is modeled besed on [2] with a map of the compressor efficiency $\eta_{kp}$

$$T_{\text{cp}} = T_{\text{atm}} + T_{\text{atm}} \frac{1}{\eta_{\text{cpp}}} \left[ \left( \frac{p_{\text{gm}}}{p_{\text{erm}}} \right)^{\frac{\lambda-1}{7}} - 1 \right] \tag{2.15}$$

where $c_p$ corresponds to the specific heat capacity of the air Excess oxygen ratio:

$$\lambda_{O2} = \frac{w_{O2,in}}{w_{O2,rct}} \tag{2.16}$$

This ratio indicates the amount of oxygen supplied to the reaction in the cathode. The excess oxygen ratio is generally regulated at $\lambda_{O_2} = 2$ to minimize the formation of stagnant steam and nitrogen films in the electrochemical zone. Values of $\lambda_{\text{O}_2} < 1$ indicate insufficient oxygen, which can severely affect battery life.

### 2.1.4 Input And Output In The Fuel Cells

The nonlinear model, based on state equations (2.2)-(2.5), encompasses four states:

$$x = [p_{O2} \quad p_{N2} \quad \omega_{\text{cp}} \quad p_{\text{sm}}]^T \tag{2.17}$$

These state equations can be formulated using the control actuator signal $v_{\text{cm}}$ and an exogenous input from the external electric load. From an electical point of view, the fuel cell model utilizes the current as an input, resulting in Equation (2.1) producing the cell voltage $v_{\text{fc}}$ and the stack voltage $v_{\text{st}}$ based on the stack current $I_{\text{st}}$ or current density $i_{\text{fc}}$. However, the choice of electric load input depends on the application. For instance, the cell voltage can serve as an input to analyze spatially distributed current density, while a resistance input may be more practical.

In the causal model discussed in this chapter, either the stack current or the stack voltage can serve as the input. Using the stack current as the input results in the dynamic behavior of the stack voltage with respect to current density and pressure conditions. Conversely, using the stack voltage as the input yields the dynamic behavior of the stack current, representing the fuel cell system's performance conditions. This dynamic interaction between current and voltage inputs is crucial for accurately modeling and understanding the performance of the fuel cell system, as also demonstrated in dynamic models for battery cells [6] .

## 2.2 Fuel-cell Linearized Model

### 2.2.1 Linearization principle

A linear model provides an estimate of how a nonlinear system behaves near a given operating state or a trajectory. Whether a system governed by a differential equation :

$$\dot{x} = f(x, u) \quad x \in \mathbb{R}^n, \quad u \in \mathbb{R}^m \tag{2.18}$$

(2.18) is called the state equation. Sometimes we add to (2.18) an output equation of the form:

$$y = h(x, u) \quad y \in \mathbb{R}^p \tag{2.19}$$

A special case of (2.18) is the control affine form that is rewritten as:

$$\dot{x} = f(x) + g(x)u \tag{2.20}$$

The behavior near the equilibrium of the nonlinear system is equivalent to that of the linear system around this point.

- If the linear model is asymptotically stable (real parts of the poles are strictly negative) then the corresponding equilibrium of the nonlinear system is locally stable.
- If the linear model is unstable then the corresponding equilibrium of the nonlinear system is unstable.

We need first to linearize the system (2.20) around the supposed operating point. here $x = 0$ at $u = 0$, thus

$$\begin{aligned} \dot{x} &= f(0) + \frac{\partial}{\partial(x,u)}[f(x) + g(x)u]_{\substack{x=0 \\ u=0}} \begin{bmatrix} x-0 \\ u-0 \end{bmatrix} \\ \dot{x} &= \left.\frac{\partial f}{\partial x}\right|_{x=0} x + g(0)u \end{aligned} \tag{2.21}$$

Then, the linear approximation of (2.20) is:

$$\dot{x} = Ax + Bu \quad \text{with} \quad A = \left.\frac{\partial f}{\partial x}\right|_{x=0}, B = g(0) \tag{2.22}$$

### 2.2.2 Linearization Methodology

The fuel-cell system nonlinear model was linearized around its nominal operating point, defined by the two variables $I_{st}^* = 220\text{A}$ and $\lambda_{O_2}^* = 2$. The corresponding equilibrium states and control can be determined by equilibrium condition, either analytically by solving a nonlinear static equation system for the state

variables, or, more practically, numerically by perturbating the system states around the equilibrium. The numerical method was used in this work. The corresponding linear model is given by :

$$\dot{z} = Az + B_c w_c + B_d w_d \tag{2.23}$$

$$y = Cz + D_d w_d \tag{2.24}$$

where $z = x - x_{eq}$, $w_c = v_{cm} - v_{cm}^*$ and $w_d = I_{st} - I_{st}^*$ are respectively the translated state, control and disturbance. $y = \lambda_{O_2} - \lambda_{O_2}^*$ is the translated output, namely the performance variable.

The matrices $A$, $B_c$ and $B_d$represent the state matrix, the control-to-state and the disturbance-to-state matrix, respectively. $C$ and $D_d$ map the state vector and the disturbance variable to the output. We note that $y$ is independent of the control $w_c$.

The numerical values of the aforementioned variables are given as follows:

$$x_{eq} = \begin{pmatrix} 17965.4 \\ 135358.3 \\ 220266.6 \\ 8743.03 \end{pmatrix} \tag{2.25}$$

$$A = \begin{pmatrix} -9.98306 & -6.49232 & 6.51673 & 18.06531 \\ -23.96414 & -27.87089 & 24.51534 & 13.60639 \\ 20.43814 & 20.43814 & -21.6952 & 83.27485 \\ 0 & 0 & -0.050844 & -7.01441; \end{pmatrix} \tag{2.26}$$

$$B_c = \begin{pmatrix} -0 \\ 0 \\ 0 \\ 365.7073 \end{pmatrix} \tag{2.27}$$

$$B_d = \begin{pmatrix} -289.8507 \\ 0 \\ 0 \\ 0 \end{pmatrix} \tag{2.28}$$

$$C = \begin{pmatrix} -0.0001 & -0.0001 & 0.0001 & 0 \end{pmatrix} \tag{2.29}$$

$$D_d = -0.009 \tag{2.30}$$

## 2.3 Model validation

### 2.3.1 Simulation around an operating point close to the reference

The simulation results for both nonlinear and linearized model are depicted in figure 2.2. It is shown that the linearized model is quite representative for the nonlinear model, for almost all the states. This is due to the fact that, in one hand, the system is simulated around an operating point close to the reference point used for the linearization, and in the other hand that state was initialized with values close to the equilibrium.

In analyzing the behavior of $(\lambda_{O_2})$ , several key observations emerge. Initially, there is a noticeable upward trend in $\lambda_{O_2}$ within both models until reaching $t = 0.5$ seconds. This observed increase in $\lambda_{O_2}$ implies a corresponding escalation in pressures within the simulated fluid flow pathway. Subsequently, as time progresses, a convergence phenomenon becomes apparent, the pressure in both models begins to stabilize, ultimately converging towards a shared value By t = 2 seconds. This convergence towards a common pressure level suggests a remarkable alignment in the behavior of the linear and non-linear models. Despite their inherent mathematical differences, both models demonstrate synchronized or symmetrical behavior in representing the evolution of pressure over time when operating close to the reference operating point.

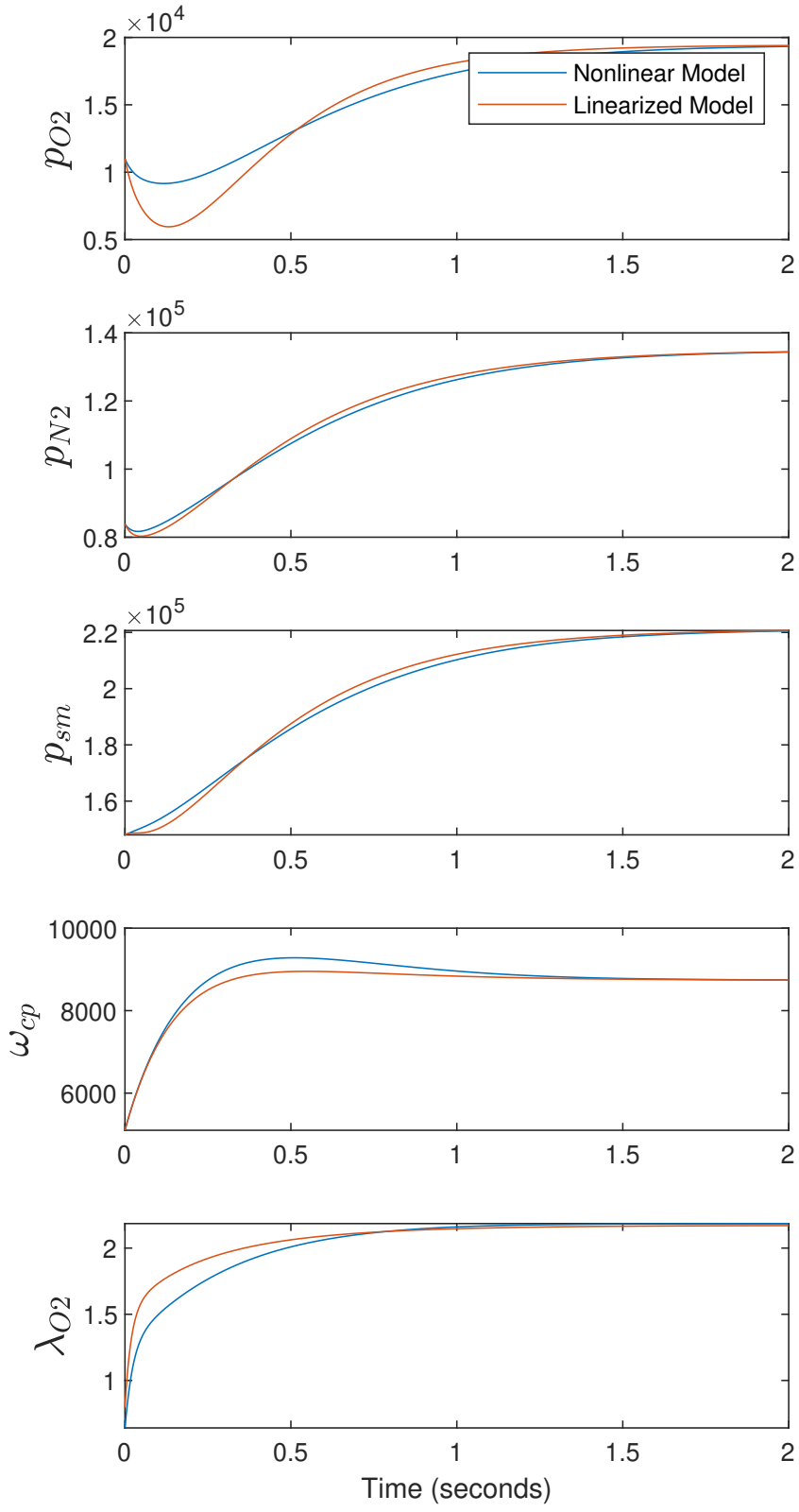




Figure 2.2: Response of the Nonlinear & Linearized Models for a fixed operating point

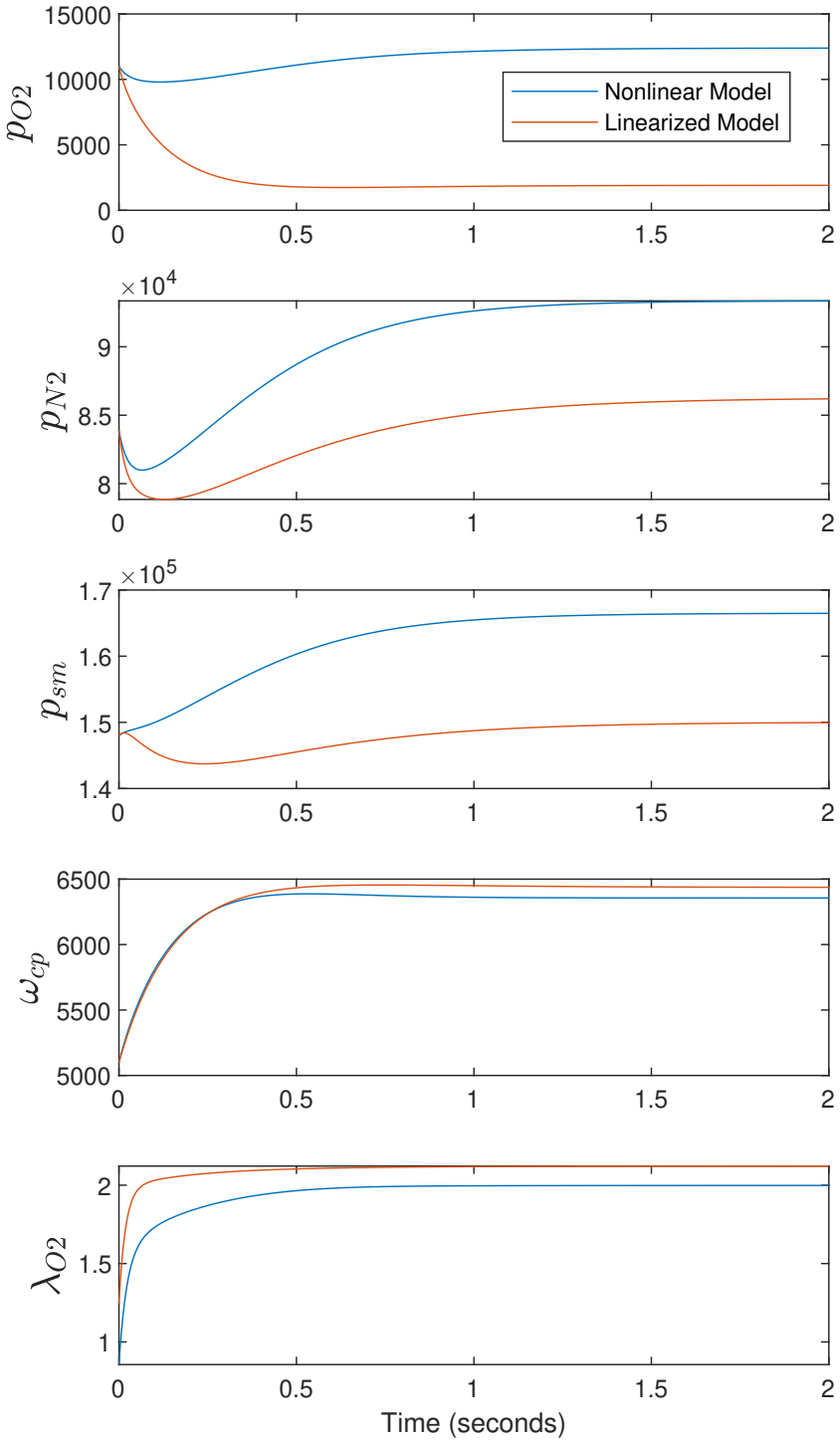


Figure 2.3: Response of the Nonlinear & Linearized Models for a different operating point

### 2.3.2 Simulation around an operating point far from the reference

The simulation results shown in figure 2.3 highlight the incapacity of the linear model to accurately simulate the behavior of the fuel cell when operating far from the reference point. This discrepancy was particularly evident, showing significant deviations between the behaviors predicted by the linear and non-linear models.

For the compressor speed dynamics, this difference is slight, with a relative error of approximately 2%. However, it becomes more pronounced for the supply manifold and nitrogen pressure dynamics, where the relative error is around 10%. For the oxygen pressure, the error is very large, and the linear model fails completely to predict the oxygen pressure behavior. This can be attributed to the strong nonlinearities present in the oxygen pressure dynamics, in contrast to the compressor speed dynamics, which exhibit more linear-like behavior.

In summary, we can conclude that the linear model is inadequate for simulating the fuel cell's behavior under conditions far from the reference operating point. The non-linear model, on the other hand, provides a more accurate representation, especially for the oxygen pressure dynamics, where nonlinearities are significant.

### 2.3.3 Conclusion

This chapter provides a detailed overview of fuel cell modeling, specifically focusing on developing a simplified model (4 states) for the PEMFC system and emphasizing the importance of linearization of the nonlinear model around a given operating mode. The simulation results for both linearized and nonlinear models demonstrate the effectiveness of the linearized model in approximating the behavior of the nonlinear model, especially when operating near the linearization point. However, it is crucial to recognize that the linearized model may not capture the complexity of the nonlinear system under different operating points, leading to significant deviations between the models. This underscores the limitations of relying solely on linear models and the importance of considering nonlinearity in system dynamics. Overall, this chapter provides a comprehensive and in-depth perspective on fuel cell modeling, with a specific emphasis on the stack model, and highlights the potential of the linearized model in approximating system behavior near the linearization point. Building on this foundation, the next chapter will explore the

flatness control of the fuel cell, addressing further aspects of system control and performance optimization essential for enhancing overall efficiency and response.

# Chapter 3

# Flatness Control of The FC air-feed subsystem

## 3.1 Introduction

Efficient fuel cell operation relies on precise control of the oxygen excess ratio, crucial for performance and longevity. This chapter explores flatness-based control applied to a linearized model of the fuel cell's oxygen excess ratio, focusing on trajectory planning. Flatness-based control simplifies design by transforming the control problem into a flat output space, allowing for easy implementation of control laws. The chapter covers:

- Theoretical foundations of flatness-based control for linear systems.
- Application of this control method to the linear and nonlinear model of the fuel cell.
- Advantages of incorporating trajectory planning to ensure desired system behavior.

Simulation results validate the approach, demonstrating its effectiveness in maintaining optimal oxygen excess ratios.

## 3.2 Flatness Control

Flatness control is a control strategy that is based on the concept of differential flatness, which considers a system to be differentially flat if there exists a set of independent variables, known as flat outputs, such that all other system variables, including the inputs, can be expressed as functions of the flat output and a finite number of its successive time derivatives. This property of differential flatness is mathematically represented by a set of equations, wherein a nonlinear system is described by state and output equations:

$$x = f(x, u) \qquad x \in \mathbb{R}^n, \quad u \in \mathbb{R}^m \tag{3.1}$$

$$y = h(x) \qquad y \in \mathbb{R}^m \tag{3.2}$$

The system is differentially flat if the state variables $x$ and the control inputs $u$ can be expressed in terms of a set of flat outputs $y_f$ and their derivatives:

$$y_f = \psi_f(x, u, \dot{u}, \ldots, x^{(r)}) \tag{3.3}$$

$$x = \psi_x(y_f, \dot{y_f}, \ldots, y_f^{(\alpha)}) \tag{3.4}$$

$$u = \psi_u(y_f, \dot{y_f}, \ldots, y_f^{(\alpha+1)}) \tag{3.5}$$

This property of differential flatness allows for a transformation of the system dynamics into a linear form, enabling more efficient control design and handling of constraints. [1]

## 3.3 Flatness of the Linear Satate space Representation

Since the introduction of Kalman's state space model of linear systems, the most common form for linear dynamic systems is a first-order vector differential equation. In the single input case this is given as follows:

$$\dot{x} = Ax + bu, \quad x \in \mathbb{R}^n, \quad u \in \mathbb{R} \tag{3.6}$$

$A$ and $b$ being, respectively, an $n \times n$ and $n \times 1$ constant matrices. Note that the characteristic

polynomial of the constant matrix $A$, written with respect of the complex variable $s$, is given by:

$$s_n + \alpha_{n-1}s_{n-1} + \cdots + \alpha_1 s + \alpha_0$$

Let the transformation of the form, $z = Tx$, in spatial coordinates, where $T$ is the stated rank of the Kalman controllability matrix:

$$z = \Lambda z + \gamma w, \quad \Lambda = TAT^{-1}, \quad \gamma = Tb \tag{3.7}$$

$$\Lambda = \begin{bmatrix} 0 & 0 & \cdots & 0 \\ 0 & \ddots & & \vdots \\ 0 & & \ddots & 0 \\ 1 & 0 & \cdots & -\alpha_{n-1} \\ 0 & \ddots & & \vdots \\ \vdots & & \ddots & 0 \\ 0 & 0 & \cdots & -\alpha_1 \\ 0 & 0 & \cdots & -\alpha_0 \end{bmatrix}, \quad \gamma = \begin{bmatrix} 1 \\ 0 \\ \vdots \\ 0 \\ 0 \end{bmatrix}$$

The state coordinate $f = z_n$, fully parameterizes both the input $u$ and the altered state $z$, and consequently the original variables $x$. It does, in fact, verify that the input $u$ and the modified variables can be expressed in terms of $f$ and a limited number of its time derivatives.

$$z_{n-1} = \dot{f} + \alpha_{n-1}f \tag{3.8}$$

$$z_{n-2} = \ddot{f} + \alpha_{n-1}\dot{f} + \alpha_{n-2}f \tag{3.9}$$

$$\vdots$$

$$z_1 = f^{(n-1)} + \alpha_{n-1}f^{(n-2)} + \cdots + \alpha_1 f \tag{3.10}$$

$$u = f^{(n)} + \alpha_{n-1}f^{(n-1)} + \cdots + \alpha_0 f \tag{3.11}$$

In matrix notation, this set of relations read is

$$\begin{pmatrix} f \\ \dot{f} \\ \ddot{f} \\ \vdots \\ f^{(n-1)} \end{pmatrix} = \begin{pmatrix} \lambda \\ \lambda A \\ \vdots \\ \lambda A^{n-1} \end{pmatrix} x + \begin{pmatrix} 0 & 0 & \cdots & 0 \\ \lambda B & 0 & \cdots & 0 \\ \lambda AB & \lambda B & \cdots & 0 \\ \vdots & \vdots & \ddots & \vdots \\ \lambda A^{n-2}B & \lambda A^{n-3}B & \cdots & \lambda B \end{pmatrix} \begin{pmatrix} u \\ \dot{u} \\ \vdots \\ u^{(n-2)} \end{pmatrix}$$

Proposition 2.4.1 The flat output of the linear controllable system with the state space form given by (3.6) is given, modulo a constant factor, by the linear combination of the states obtained from the last row of the inverse of the Kalman controllability matrix $\left[B, AB, \ldots, A^{n-1}B\right]$ i.e. [3]

$$y_f = \begin{bmatrix} 0 & 0 & \cdots & 1 \end{bmatrix} \left[ b \quad Ab \quad \cdots \quad A^{n-1}b \right]^{-1} x \tag{3.12}$$

## 3.4 Flatness of the Linear Model of the Fuel cell

We recall that the FC system linear model is given in the form

$$\dot{z} = Az + B_c w_c + B_d w_d \tag{3.13}$$

$$y = Cz + D_d w_d \tag{3.14}$$

The system has two inputs, one control and one disturbance variables. In flatness system theory the disturbance is seen as a system input and also as a component of the flat output vector, this yields the following proposition:

**Proposition 1** *A flat output for the system (3.13) is given by*

$$y_f = \begin{bmatrix} y_{f1} \\ y_{f2} \end{bmatrix} = \begin{bmatrix} w_d \\ C_f z \end{bmatrix}$$

where $C_f$ is given by

$$C_f = \begin{bmatrix} 0 & 0 & \cdots & 1 \end{bmatrix} \left[ B_c \quad AB_c \quad \cdots \quad A^{n-1}B_c \right]^{-1} \tag{3.15}$$

**Proof 1** *We repeatedly differentiate $y_{f2}$ three times with respect to the time, and we will see that $w_c$ vanishes always.*

$$y_{f2} = C_f z \tag{3.16}$$

$$\dot{y}_{f2} = C_f A z + \cancelto{0}{C_f B_c w_c} + C_f B_d w_d \tag{3.17}$$

$$\ddot{y}_{f2} = C_f A^2 z + \cancelto{0}{C_f A B_c w_c} + C_f A B_d w_d + C_f B_d \dot{w}_d \tag{3.18}$$

$$\dddot{y}_{f2} = C_f A^3 z + \cancelto{0}{C_f A^2 B_c w_c} + C_f A^2 B_d w_d + C_f A B_d \dot{w}_d + C_f B_d \ddot{w}_d \tag{3.19}$$

$$\tag{3.20}$$

*This makes it possible to write $z$ in terms of $y_f$ and its time derivatives as:*

$$z = \begin{bmatrix} C_f \\ C_f A \\ C_f A^2 \\ C_f A^3 \end{bmatrix}^{-1} \begin{bmatrix} y_{f2} \\ \dot{y}_{f2} - C_f B_d y_{f1} \\ \ddot{y}_{f2} - C_f A B_d y_{f1} - C_f B_d \dot{y}_{f1} \\ \dddot{y}_{f2} - C_f A^2 B_d y_{f1} - C_f A B_d \dot{y}_{f1} - C_f B_d \ddot{y}_{f1} \end{bmatrix} \tag{3.21}$$

*A fourth differentiation of $y_f$ will make $w_c$ appear as follows:*

$$y_{f2}^{(4)} = C_f A^4 z + C_f A^3 B_c w_c + C_f A^3 B_d y_{f1} + C_f A^2 B_d \dot{y}_{f1} + C_f A B_d \ddot{y}_{f1} + C_f B_d \dddot{y}_{f1} \tag{3.22}$$

*then, the control can be written in terms of $y_f$ and its time derivatives as follows which prove the statement.*

$$w_c = [C_f A^3 B_c]^{-1} [y_{f2}^{(4)} - C_f A^4 z - C_f A^3 B_d y_{f1} - C_f A^2 B_d \dot{y}_{f1} - C_f A B_d \ddot{y}_{f1} - C_f B_d \dddot{y}_{f1}] \tag{3.23}$$

The flat matrix $C_f$ of the linear fuel cell defined by the matrices (2.26)-(2.28) is given by

$$C_f = \begin{pmatrix} -0.2007 \\ 0.0743 \\ 0.0314 \\ 0 \end{pmatrix}$$

**Remark 1** *The expression (3.23) is called the feed-forward control, it allows to track any trajectory $y_f$ of class $C^4$ provided it respects the initial condition of the system.*

## 3.5 Trajectory Planning

### 3.5.1 Polynominal Trajectory Generation

Multiple-boundary type trajectories are commonly employed to guide stable reference outputs from an initial state $y_f(0)$ to a final state $y_f(t_f)$ within a specified time $T_p$. The degree of this polynomial trajectory depends on the relative degree of the system. In practice, it is often preferable to use "stop-stop" trajectories, where the first and second derivatives are assumed to be zero at the beginning and the end to reduce computation time in the planning phase. During the planning stage, it is important to ensure the following constraints: transitioning between two equilibrium points, taking into account the bounded control between 0 and $\overline{v}_{cm}$ (an approximated defined value). In the context of the fuel cell, only $y_{f2}$ is planned, while $y_{f1}$ is a measured disturbance that is supposed sufficiently differentiable with perfectly known derivatives. The planned trajectory of $y_{f2}$ can be defined as :

$$y^*_{f2}(t) = \sum_{j=0}^{5} p_j t^j \tag{3.24}$$

where $p_j$ are constants determined to guarantee the consistency of the boundary values of the planned trajectory.

### 3.5.2 Trajectory generation using Filters

In the context of trajectory generation within flatness control, utilizing a step signal in conjunction with filters is a viable approach. While convergence to the target is asymptotic (achieved in finite time using polynomials), filters can perform exceptionally well, especially when dealing with variable references. The core principle involves designing a filter with a specific order, typically chosen to ensure the output can be differentiated a sufficient number of times. This can also be achieved by serially connecting multiple first-order filters. The time constant is set according to the desired response speed.

Alike in polynomial trajectory generation, using filters, the differentiation is straight-forward as it consists to multiply the output by $s$ in the Laplace domain, causality is not violated, as the denominator of the filter is of order greater than or equal to the number of differentiations needed.

Figure (3.1) illustrates the transfer function of the filter used for planning. The schema is generalized to encompass the generation of $y_f^*$ and its derivatives.

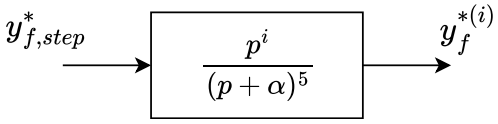


Figure 3.1: Trajectory Planning using filters

## 3.6 Simulation

In our research, we focus on controlling the flat output of the fuel cell system to precisely regulate the trajectory of the oxygen excess ratio denoted as $\lambda_{O_2}$. Initially, we set $y_{f2}^{init} = 0$ and ultimately adjust it to $y_{f2}^{fin} = 0.01$, targeting a final $\lambda_{O_2}^{fin}$ value of 2.3. The reduced nonlinear model, as proposed by [**?**], is characterized by its complexity and high nonlinearity, which pose significant challenges in the control synthesis, particularly for flat control design. To facilitate more the control design, our flat control was based on the linear model of the fuel cell around its nominal operating point characterized by $I_{st}^{nom} = 220\text{A}$ and $v_{cm}^{nom} = 175\text{V}$.

In the simulation, the output current is considered constant and equal to its nominal value 220A, based on which the linearization was performed. We note that we could consider any trajectory of $I_{st}$, the only conditions is that it must be perfectly known, and differentiable a sufficient number of times, so

that the control is smooth. The closed-loop dynamics of the system in the flat space can be described by the following equation:

$$(p^2 + 2\xi\omega_0 p + \omega_0^2)(p + p_3)(p + p_4) = a_0 + a_1 p + a_2 p^2 + a_3 p^3 \tag{3.25}$$

The coefficients are defined as follows:

$$a_0 = \omega_0^2 \cdot p_3 \cdot p_4 \tag{3.26}$$

$$a_1 = 2\xi\omega_0 \cdot p_3 \cdot p_4 + \omega_0^2 \cdot p_4 + \omega_0^2 \cdot p_3 \tag{3.27}$$

$$a_2 = p_3 \cdot p_4 + 2 \cdot p_4 \cdot \xi\omega_0 + 2\xi\omega_0 \cdot p_3 + \omega_0^2 \tag{3.28}$$

$$a_3 = p_4 + p_3 + 2\xi\omega_0 \tag{3.29}$$

We use the following parameter values:

$$\xi = 0.7 \tag{3.30}$$

$$\omega_0 = 10 \tag{3.31}$$

$$p_3 = 500 \tag{3.32}$$

$$p_4 = 500 \tag{3.33}$$

The shematic diagram of figure (3.2) illustrates the flatness control of the fuel cell system and its operation. The graphical representation aids in understanding the control strategy, and evaluating its complexity.

In this study, the simulation process for the linear model is divided into two distinct parts. First, we perform the simulation using the linearized model to validate the flat control strategy. This initial phase ensures that the control design works effectively under linear assumptions. Next, we conduct simulations using the nonlinear model of the system to evaluate the robustness of the controller in the presence of nonlinearities. This two-step approach allows us to verify the control strategy in an idealized linear context before testing its performance under more realistic conditions that include nonlinear dynamics.

The results presented in this work demonstrate the effectiveness of the control strategy in the lin-

Table 3.1: Parameters of the FC used in the simulation

| | Variable | Value |
|---|---|---|
| $\rho_{m,dry}$ | membrane dry density | 0.002 kg/cm$^3$ |
| $M_{m,dry}$ | membrane dry equivalent weight | 1.1 kg/mol |
| $t_m$ | membrane thickness | 0.01275 cm |
| $n$ | number of cell in fuel cell stack | 381 |
| $A_{fc}$ | fuel cell active area | 280 cm$^2$ |
| $d_c$ | compressor diameter | 0.2286 m |
| $J_{cp}$ | compressor and motor inertia | $5 \times 10^{-5}$ kg$^2$ |
| $V_{an}$ | anode volume | 0.005 m$^3$ |
| $V_{ca}$ | cathode volume | 0.01 m$^3$ |
| $V_{sm}$ | supply manifold volume | 0.02 m$^3$ |
| $V_{rm}$ | return manifold volume | 0.005 m$^3$ |
| $C_{D,rm}$ | return manifold throttle discharge coefficient | 0.0124 |
| $A_{T,rm}$ | return manifold throttle area | 0.002 m$^2$ |
| $k_{sm,\text{ out}}$ | supply manifold outlet orifice constant | $0.3629 \times 10^{-5}$ kg/(s $\cdot$ Pa) |
| $k_{ca,\text{ out}}$ | cathode outlet orifice constant | $0.2177 \times 10^{-5}$ kg/(s $\cdot$ Pa) |

earized model and provide insights into its robustness when applied to the nonlinear model. Additionally, they clarify the relationship and differences between the proposed results and the final obtained results, offering a deeper understanding of the controller's performance under various operational conditions. This approach ensures that the control strategy is not only effective in ideal conditions but also capable of handling the challenges.

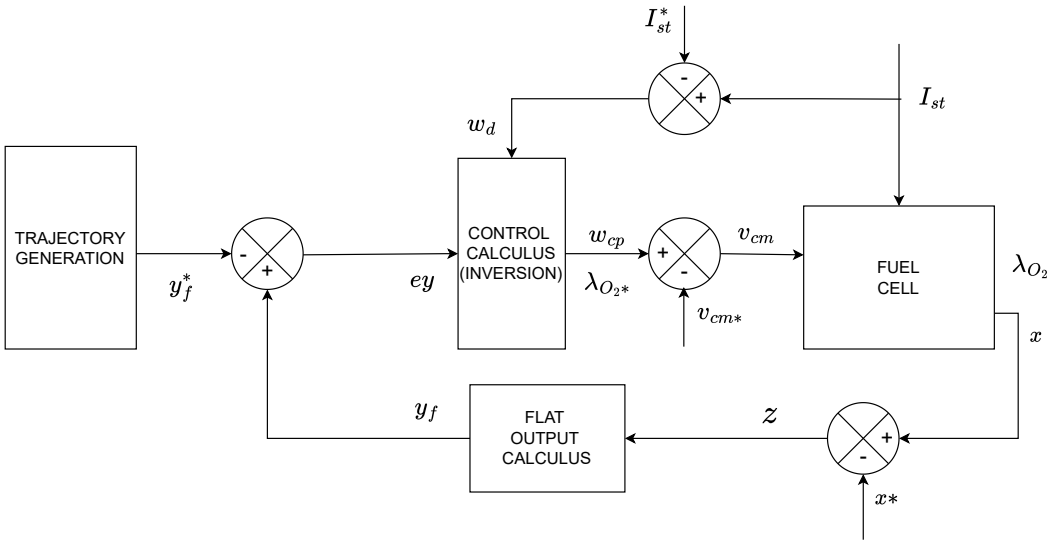


Figure 3.2: Fatness control of Fuel cell Model

### 3.6.1 Fltaness-Based Control of the Linear Fuel cell

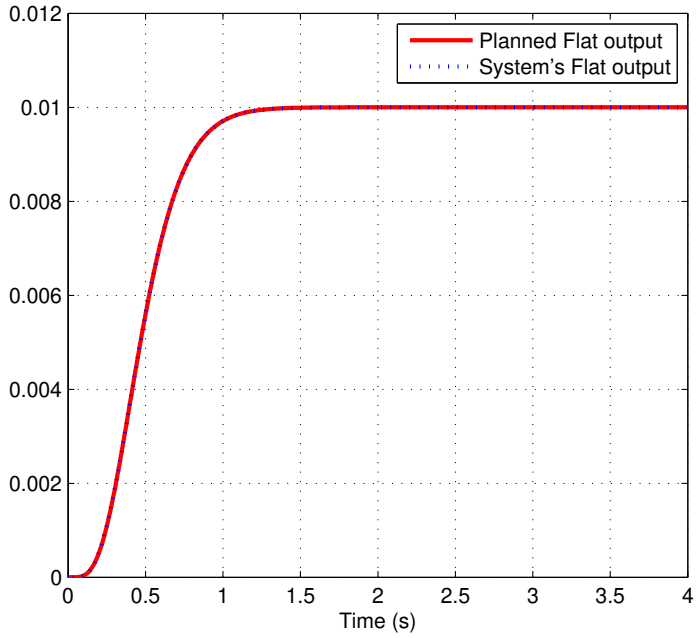


Figure 3.3: Flat output lineair model

With the linear model, the reference flat output $y_{f2}$ is designed to converge smoothly within approximately 1 second, starting from zero and reaching 0.01. In the original domain, this corresponds to $\lambda_{O2}$ increasing from 2 to 2.3. The flat trajectory is meticulously planned to avoid overshoot, facilitated by the filter's design, which excludes complex poles. However, the trajectory of $\lambda_{O2}$, a direct outcome of $y_{f2}$'s planning, exhibits noticeable overshoot, which is acceptable for the fuel cell's health. Crucially, the planned trajectory is flawlessly tracked from start to finish, showcasing the efficacy of flat control with trajectory planning capabilities.

Figure (3.4) illustrates the behavior of the four key states: oxygen pressure, nitrogen pressure, SM pressure, and CM speed. Each state exhibits an initial overshoot before stabilizing at its respective steady-state value. Despite these overshoots, the flat output control effectively tracks the desired signals, achieving precise stabilization without oscillations or deviations. This underscores the robustness and accuracy of the flatness control method in managing and stabilizing the various states of the fuel cell system. Furthermore, despite the initial overshoots, all states accurately converge to their equilibrium points, demonstrating the precision and stability of the linear flatness. This indicates that the flatness control approach is highly effective in ensuring the fuel cell system's states reach and maintain their

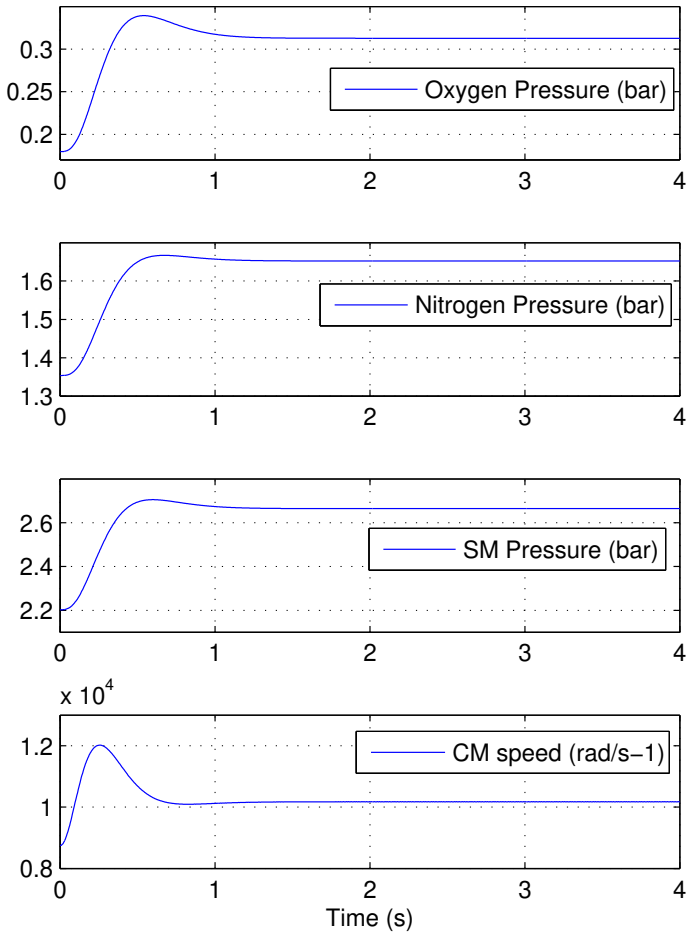


Figure 3.4: states lineair control

desired values with great performance.

### 3.6.2 Simulation with the nonlinear Fuel-cell model

After conducting simulations using the linearized fuel cell model, we applied linear-flatness-based closed-loop control to the nonlinear model of the fuel cell. As shown in Figure (3.6), unlike the linear case, the planned trajectory is no longer well tracked, resulting in persistent tracking errors and steady-state deviations observed in both the flat signal and the $\lambda^*_{O2}$ curve. This discrepancy demonstrates the inability of linear flatness-based control to effectively address the regulation objective in the presence of significant nonlinearities.

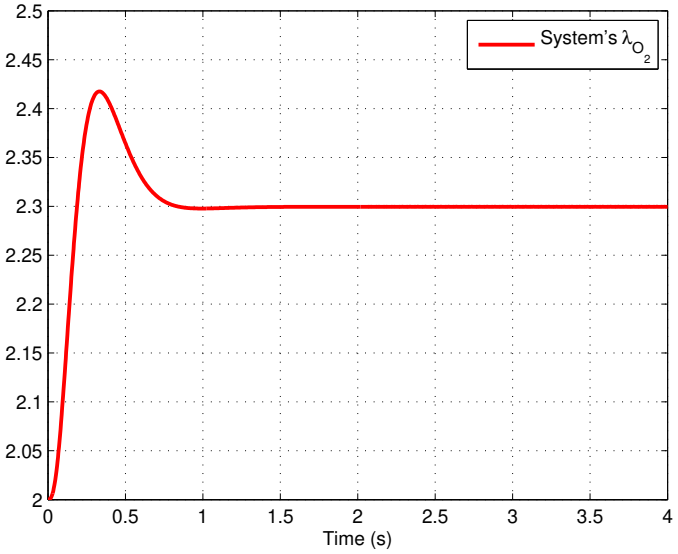


Figure 3.5: lamda O2 lineair model

This result can be interpreted by the fact that nonlinearities introduce system uncertainties that fundamentally alter the dynamics of the fuel cell. These uncertainties can lead to deviations from the idealized linear behavior assumed by the flatness-based control approach. Consequently, a more robust control strategy capable of accommodating these nonlinear effects may be necessary to achieve improved performance and regulation accuracy.

### 3.6.3 Modified Linear Flatness-based Control of PEMFC

To overcome the limitations of linear flatness-based control, we enhanced the architecture by integrating a Proportional-Integral (PI) controller. This PI controller incorporates the system output error $\lambda_{O_2}$ into the flat control framework, leading to significant improvements in maintaining the desired $\lambda^*_{O2}$ trajectory with higher precision. This adjustment ensures more accurate regulation of oxygen flow throughout the fuel cell system.

Specifically, the expected trajectory for $\lambda_{O_2}$ is initially determined based on the planned flat output derived from the linear fuel cell model. Subsequently, the calculation of the flat output from measurements obtained from the nonlinear system is corrected using an additive term generated by the PI controller. The PI controller utilizes the error signal between the measured $\lambda_{O_2}$ and its expected trajectory, calculated from the linear model-based flat output.

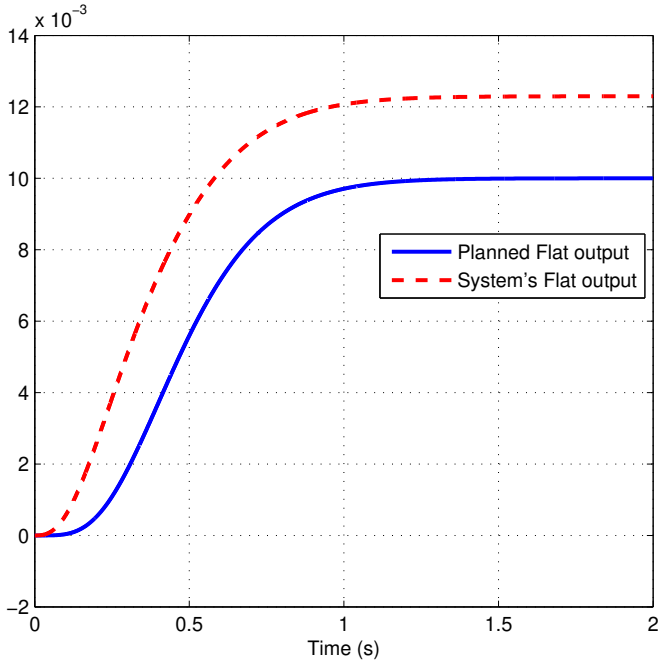


Figure 3.6: Flat output signals of the nonlinear model

With this enhancement, the system effectively tracks the expected $\lambda_{O_2}$ trajectory, thereby optimizing the operation towards achieving the target point at $\lambda = 2.3$. This approach facilitates successful stabilization at the set point without significant oscillations or deviations.

### 3.6.4 Conclusion

In conclusion, the incorporation of the output error in the flatness-based control architecture via PI controller has proven instrumental in addressing the challenges posed by nonlinearities in the fuel cell system. By actively correcting deviations between expected and measured $\lambda_{O_2}$ values, the enhanced control strategy achieves robust and precise regulation, crucial for stable operation and performance optimization. Moving forward, further refinements and possibly adaptive control techniques could be explored to continuously enhance the system's ability to maintain optimal conditions and adapt to varying operational demands effectively. This adaptive approach ensures continued reliability and efficiency in managing oxygen flow within the fuel cell system, supporting its long-term operational stability and performance goals.

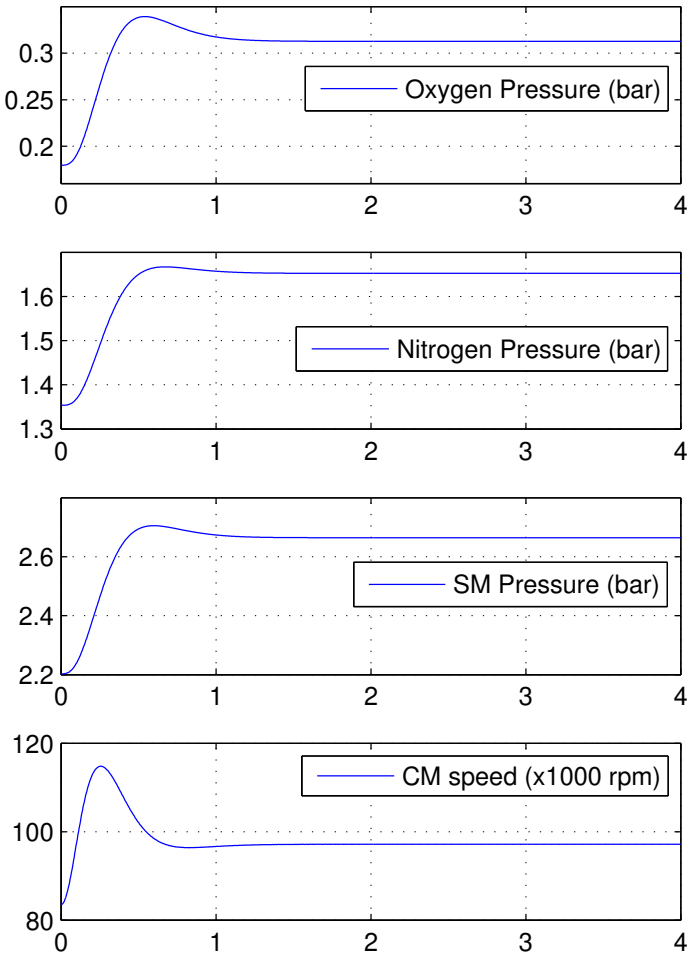


Figure 3.7: state signals of the nonlinear model

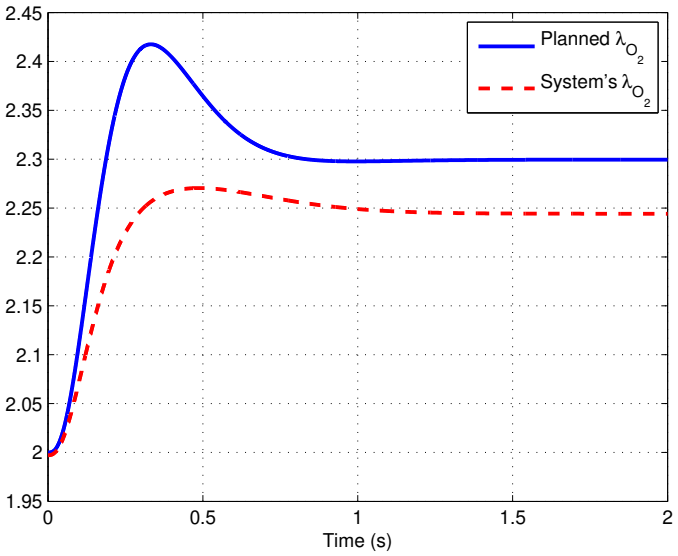


Figure 3.8: $lambda_{O2}$ trajectory in the nonlinear model

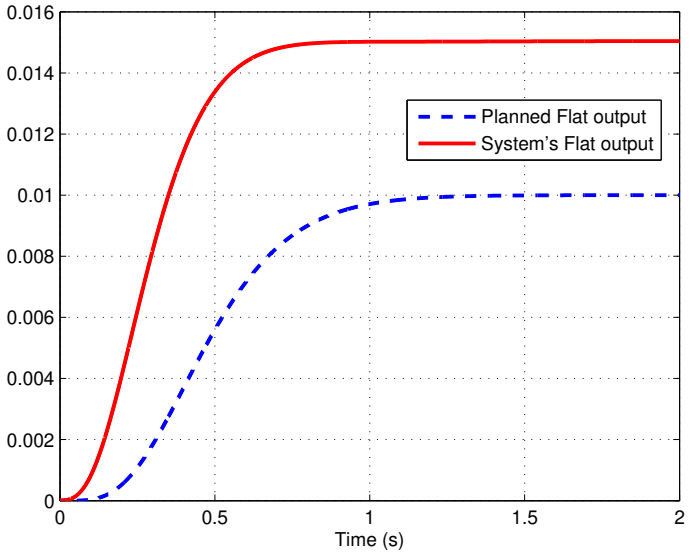


Figure 3.9: Flat output signal with the modified Flatness-based control

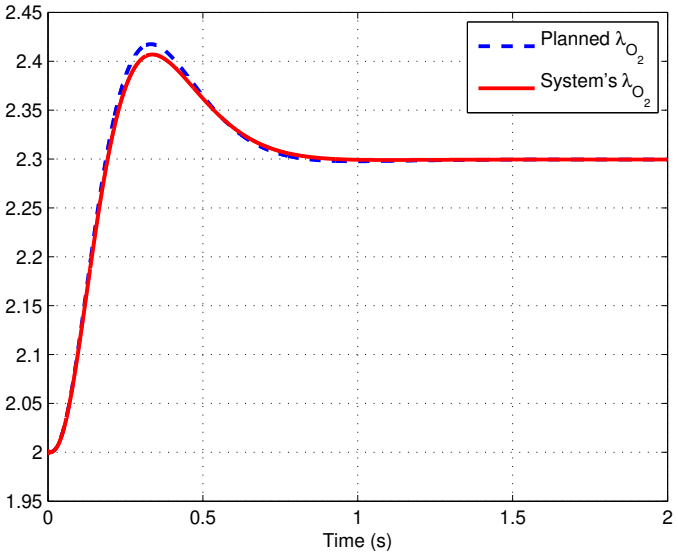


Figure 3.10: $\lambda_{O2}$ signal with the modified flatness-based control

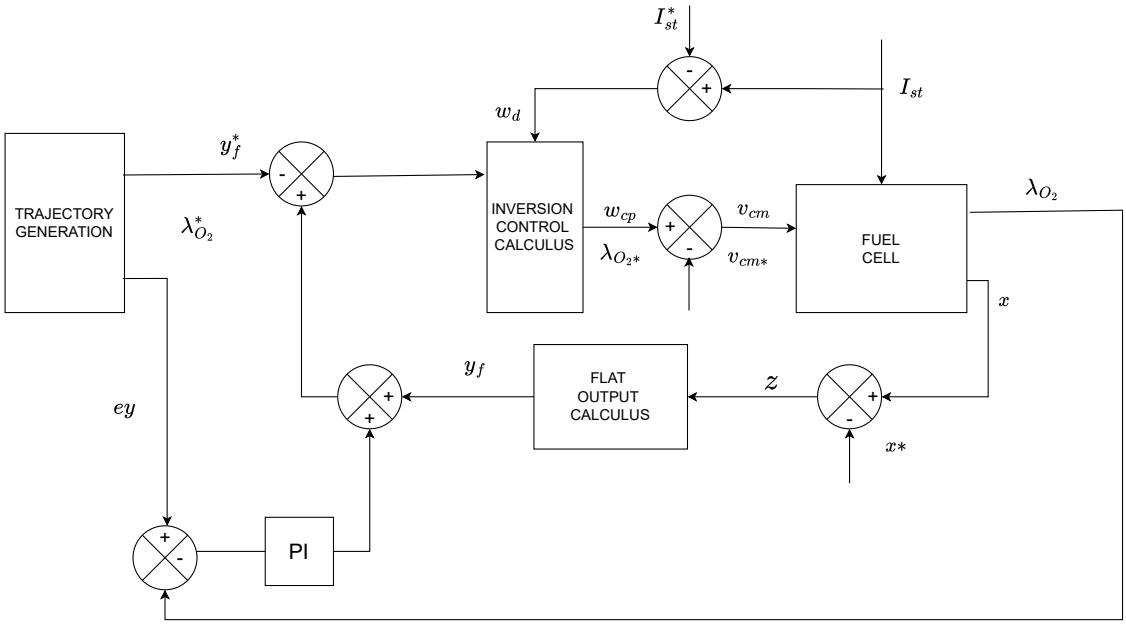


Figure 3.11: Fatness control of Fuel cell Model with Flat Output Correction

# General conclusion

In this study, we focused on developing a flatness-based control strategy for regulating the oxygen excess ratio ($\lambda_{O2}$) in a fuel cell system. Initially, we established a reduced four-state model and its linearized version around a nominal operating point, providing a foundational understanding of the system's dynamics under small perturbations. Comparative analyses between the linear and nonlinear models at different operating points highlighted significant deviations in system response, emphasizing the impact of nonlinearities on control performance.

Our initial application of flatness control based on the linear model demonstrated perfect tracking of the desired $\lambda_{O2}$ trajectory. However, when applied to the full nonlinear model, substantial tracking errors emerged, revealing the limitations of linear-based approaches in handling real-world complexities.

To address these challenges, we enhanced the control strategy by integrating a Proportional-Integral (PI) controller into the flatness architecture. This adaptation effectively incorporated the output $\lambda_{O2}$ error into the control loop, significantly improving precision and stability in regulating $\lambda^*_{O2}$.

This study underscores the critical role of robust control strategies in optimizing fuel cell performance across varying operational conditions. Future research directions may explore advanced control techniques, such as adaptive and predictive control, to further enhance the system's ability to maintain optimal operation and meet stringent performance targets in practical applications. By bridging theoretical modeling with practical control design, this work contributes to the ongoing efforts in advancing fuel cell technology for sustainable energy solutions.

# Bibliography


[1] Guillaume Allibert, Estelle Courtial, and Youssoufi Touré. A flat model predictive controller for trajectory tracking in image based visual servoing. *IFAC Proceedings Volumes*, 40(12):993–998, 2007.

[2] Debabrata Das and T Nejat Veziroğlu. Hydrogen production by biological processes: a survey of literature. *International journal of hydrogen energy*, 26(1):13–28, 2001.

[3] M. Fliess and J. Levine. *Theorie et Pratique des Systemes Plats*. CRC Press, Boca Raton, FL, 2004.

[4] Klaus Wolfgang Friede. *Modélisation et caractérisation d'une pile à combustible du type PEM*. PhD thesis, Vandoeuvre-les-Nancy, INPL, 2003.

[5] WB Gu, Chao-Yang Wang, and BY Liaw. numerical modeling of coupled electrochemical and transport processes in lead-acid batteries. *Journal of The Electrochemical Society*, 144(6):2053, 1997.

[6] Mohamed Harmouche, Imad Matraji, Salah Laghrouche, and Mohammed El-Bagdouri. Homogeneous higher order sliding mode control for pem fuel cell. In *2012 12th International Workshop on Variable Structure Systems*, pages 161–166. IEEE, 2012.

[7] Kamran Javed, Rafael Gouriveau, Noureddine Zerhouni, and Daniel Hissel. Pem fuel cell prognostics under variable load: A data-driven ensemble with new incremental learning. 04 2016.

[8] Amel Lachichi. *Modélisation et stabilité d'un régulateur hybride de courant-Application aux convertisseurs pour pile à combustible*. PhD thesis, Université de Franche-Comté, 2005.

[9] Ross A Lemons. Fuel cells for transportation. *Electric Vehicle Developments;(UK)*, 8(4), 1989.

[10] Imad Matraji. *Contribution à la commande non linéaire robuste des systèmes d'alimentation en air des piles à combustible de type PEM*. PhD thesis, Université de Technologie de Belfort-Montbeliard, 2013.

[11] Fahed Mekhalfia. Modelisation des piles a combustible application a l'entrainement du moteur asynchrone. Master's thesis, Université Mohamed Boudiaf - M'sila, 2008.

[12] Hossein Pourrahmani, Adel Yavarinasab, Majid Siavashi, Mardit Matian, et al. Progress in the proton exchange membrane fuel cells (pemfcs) water/thermal management: From theory to the current challenges and real-time fault diagnosis methods. *Energy Reviews*, 1(1):100002, 2022.

[13] Jay T Pukrushpan, Anna G Stefanopoulou, and Huei Peng. *Control of fuel cell power systems: principles, modeling, analysis and feedback design*. Springer Science & Business Media, 2004.

[14] Adam Z Weber, Sivagaminathan Balasubramanian, and Prodip K Das. Proton exchange membrane fuel cells. In *Advances in Chemical Engineering*, volume 41, pages 65–144. Elsevier, 2012.

[15] Baroud Zakaria, Gazzam Noureddine, Benalia Atallah, and Ocampo-Martinez Carlos. Algebraic observer-based output-feedback controller design for a pem fuel cell air-supply subsystem. *IET Renewable Power Generation*, 12(14):1714–1721, 2018.

[16] Jianlu Zhang, Yanghua Tang, Chaojie Song, Jiujun Zhang, and Haijiang Wang. Pem fuel cell open circuit voltage (ocv) in the temperature range of 23 c to 120 c. *Journal of power sources*, 163(1):532–537, 2006.